

Spatial Coordinates in Interferometry Fringes

A Timeless Artwork Multipurpose Documentation

Vivi Tornari

Institute of Electronic Structure and Laser, Foundation for Research and Technology-Hellas

N.Plastira 100, Heraklion 71110, Crete, Greece

vivitor@iesl.forth.gr

Abstract- Coherent holographic metrology provides the non-contact potential to retrieve directly from surface measurements of the spatial displacement information originating from the bulk of complex objects suffering inherent faults or physical deterioration. These damage factors endanger the structural integrity and lessen the life span of works of art, inevitably reaching the fragile and precious surface. Interferometry techniques via interference fringes offer NDT for surface authentication and impact analysis and overall quality control in order to provide a signature of precious surface responses or exempt faulted products from the production line. In this paper the 2D interferometry information is instead implemented as a NDT to prevent artworks from physical deterioration. It is proposed a structural diagnosis method via 2D spatial data derived from interference intensity profiles. Thus the paper introduces the concept to diagnose the structural condition via direct contactless interference examination of artwork surface with the prospect of timeless documentation in art conservation field.

Keywords- *Holographic Interferometry; Interferometry; Holography; Optical Metrology; Art Conservation; Quality Testing; NDT*

I. INTRODUCTION

In authentication and preservation of works of art the fundamental information to document, understand, restore and plan preventive maintenance is mostly based on short term evidence captured by the curator's "critical or trained eye" [1-3]. Documentation and restoration practice is missing quantitative accurate and repeatable methods that could enable development of efficient long-term practises.

The spatial data provided by surface illumination in structural monitoring via interferometry techniques represent a self-produced "surface-matrix" of object points that could be used as the input for timeless comparison purpose and a fingertip originality method against impact and fraud.

In this context a brief on the concept of the structural documentation, the state of the art of modern techniques involved, the principles of spatial coordinate's formation and its signature retrieval properties through comparative interferometric records are presented.

A. Object Points Infinity

Any structural object at the time of construction is defined by an infinite number of points at initial positions whereas by the aging and natural decay of structure results to their displacement from the initial position to altered positions in an ever going process. These alterations affect the structural condition that determines the preventive conservation and maintenance strategies in order to avoid artwork damage [4-6].

If the structural condition is micrometrically revealed and quantified, it can provide a "self-reference" value of a "surface-matrix" of points as first spatial data documentation

against which a multipurpose tool is obtained: from assessing impact and deterioration to originality and fraud to plan and correct maintenance and microclimate over times to come. The structural condition is traced by surface acquired spatial coordinates as they are altered throughout their aging process. Damaging actions or successful interventions are deducted upon comparison of the last to the initial-reference position of the spatial field enfolded into surface points. This is the concept that forms the subject of the paper. As this is the first paper on the use of spatial coordinates for timeless multipurpose documentation a thorough introduction to the concept is considered thereafter.

II. STATE-OF-THE-ART

The aging, either natural or induced by accidental handling or careless environmental loading, provokes structural modifications both to the surface, interfaces and the bulk of the object. These structural modifications cannot be detected by x-ray tomographic, coherent tomographic, confocal or spectroscopic imaging since none of these methods operates on spatial data basis and none of these is sensitive to spatial displacement.

X-ray radiography, x-ray computed tomography and multiplanar axial tomographic imaging visualize qualitatively non-uniformly composed material depending on the absorption proportional and beam attenuation of the object. By utilizing the physical properties of the ray an image can be developed displaying clearly, areas of different density and composition and computer assisted reconstruction is used to generate a 3D representation. The application on artworks allows developing scanning devices using greater resolution and penetrating power to allow peering inside without damaging it.

Optical coherence tomography (OCT) visualise detailed images from transparent layered surfaces in micrometer-resolution. It can generate three-dimensional images from within optical scattering media such as varnishes in a video rate. Optical coherence tomography is based on interferometry with typical wavelengths in Near IR to allow penetration into scattering medium. OCT compared to confocal microscopy can achieve better penetration depths. Depending on the properties of the light source as lasers, superluminescent diodes and ultrashort pulsed lasers Optical coherence tomography may achieve sub-micrometer resolution with wide-spectrum sources emitting over a ~100 nm wavelength range. Many scanning schemes offer broad applicability in the technique and system adaptability to harsh environments and more recently in art conservation research [7-11].

Confocal imaging aims to overcome some limitations of traditional wide-field microscopes or fluorescence microscopes by eliminating the out of focal plane signals and

creating high contrast sharp focus slices of the structure under investigation. In a conventional wide-field fluorescence microscope the entire sample is being illuminated from the light source. All parts of the specimen in the optical path are excited at the same time and the resulting fluorescence signal is detected by the microscope's photodetector or CCD. Thus it is included a large unfocused background part of the structure generating high image to noise ratios. In contrast, a confocal microscope uses point illumination and a pinhole in an optically conjugate plane in front of the detector to eliminate out-of-focus signal. Hence only light produced very close to the focal plane is detected, and the image's optical resolution, particularly in the sample depth direction, is much better compared to wide-field microscopes. However, the light from sample is severely blocked at the pinhole and increase in resolution is accompanied by decreased signal intensity with requirements for long exposures in optical tables. As only one point in the sample is illuminated at a time, 2D or 3D imaging requires scanning over a regular rectangular pattern of parallel scanning lines in the specimen. The achievable thickness of the focal plane is defined mostly by the wavelength of the used light divided by the numerical aperture of the objective lens and by the optical properties of the artwork structure. The thin optical sections provide particularly accurate 3D imaging and surface profiling of structure. Different types of confocal microscope with particular advantages and disadvantages have been developed and are either optimised for resolution or high recording speed (i.e. video capture) ^[12, 13].

Multi-spectral imaging is used to capture image data at specific frequencies across the electromagnetic spectrum extracting data outside the visible spectrum. The wavelengths may be separated by interference filters blocking or transmitting the chosen wavelengths or by the use of instruments that are sensitive to particular wavelengths, including IR. Dividing the spectrum into many bands, multi-spectral is the opposite of panchromatic which records only the total intensity of radiation on each photosensitive element or pixel. Multispectral images with more numerous bands or finer spectral resolution or wider spectral coverage may be called hyperspectral or ultra-spectral. The difference in light reflectivity makes parts of the scene more clearly depending to the filter being used and by using advanced digital image processing techniques underdrawings, hidden text and other elements can be recovered. Multispectral cameras are robust, easy to use and transportable devices allowing on-field application in harsh environments and as such have been easily accepted from the conservation community ^[14, 15].

Another range of techniques which is not based on the chemical properties of surface of the artwork but on the geometrical properties of the surface is termed photogrammetry.

Photogrammetry is used to determine the geometric properties of objects from photographic images by measuring the distance between two points that lie on a plane parallel to the photographic image plane that determines their distance on the image. If the scale s of the image is known, the measured distance is multiplied by $1/s$.

While photogrammetry is mostly used for two-dimensional measurements, the stereophotogrammetry, involves estimating the three-dimensional coordinates of points on an object. These are determined by measurements made on two or more photographic images taken from different positions according to the principles of stereoscopy.

The usual practice involves the extraction of common points on each image with a line of sight (or ray) being constructed from the camera location to the same point on the object. It is the intersection of these rays that determines the three-dimensional location of the point based on the principles of triangulation. Specially developed algorithms are used to exploit apriori knowledge of the scene allowing reconstructions of 3D coordinates from only one camera position. Photogrammetry which is used in many different fields for topographic purposes and on artworks has been introduced for shape reconstruction ^[16]. Geometrical properties can be also revealed by modern Fringe Projection techniques or structured-light 3D scanners to measure the three-dimensional shape of an object. The method lies on structured-light projection on the surface of the object. The structured by interference light patterns are then captured by a camera system. Projecting a narrow band of light onto a three-dimensionally shaped surface produces a line of illumination that appears distorted from other perspectives than that of the projector, and can be used for an exact geometric reconstruction of the surface shape (light section). A faster and more versatile method is the projection of patterns consisting of many stripes at once, or of arbitrary fringes, as this allows for the acquisition of a multitude of samples simultaneously. Seen from different viewpoints, the pattern appears geometrically distorted due to the surface shape of the object. Although many other variants of structured light projection are possible, patterns of parallel stripes are widely used. The displacement of the stripes allows for an exact retrieval of the 3D coordinates of any details on the object's surface and the displacement of any single stripe can directly be converted into 3D coordinates. The optical resolution of fringe projection methods depends on the width of the stripes used and their optical quality and it is limited by the wavelength of light. An extreme reduction of stripe width proves inefficient due to limitations in depth of field, camera resolution and display resolution. Therefore the phase shift method has been widely established using typically 10 exposures with slightly shifted stripes. The limitation of application in highly reflecting or transparent objects causes extra difficulties in case of varnished surfaces since double reflections cause the stripe pattern to be overlaid with unwanted light, entirely eliminating the chance for proper detection. Reflective or transparent cracks or cavities due to worm-tunneling, organic decayed surfaces with holes and damage due to moth-dispersion are therefore difficult to be recorded. The method is extensively used in industrial applications of large scale structures and in this context can be very useful in documentation of shape of monumental cultural objects ^[17].

The natural progressively developed dimensional changes witnessed in the surface and the bulk of layered or solid artworks as a consequence of slow but steady deterioration processes in order to be acquired presuppose use of techniques sensitive to spatial displacement. By using a laser beam to illuminate the surface of artwork, the surface displacement can be used to visualize alterations both in the bulk and in the surface. The laser interferometry techniques acquire the internal structural condition from surface reactions, causing the laser light to generate unique intensity patterns of displacement. The application does not require contacting, interacting or interfering with artwork structural condition. Since an artwork has extended life span of constant deterioration, the spatial alterations may vary from sub-metric to many multiples of micrometer range. In recent years different optical interferometry geometries have been

introduced to provide the required variety in displacement sensitivity and direction. An optical interferometer provides in-plane sensitivity for stress and strain measurements^[18, 19]. Holographic interferometry provides high out-of-plane sensitivity for deformation measurements^[20-22]. Speckle pattern interferometry provides moderated displacement sensitivity^[23-25]. Digital shearography provides sheared wave insensitivity to extraneous low-frequency displacements while the implementation of photorefractive crystals provides high resolution laboratory requirements. Thus the applicability of optical metrology in artwork research and documentation is significantly broadened^[26-30].

In the context of the paper only the interference techniques contributing to the use of spatial information as a tool to detect minor spatial displacement are hereafter considered with main emphasis to the higher sensitivity holographically modulated intensity profiles.

III. EXPERIMENTAL PRINCIPLE

The concept of “surface-matrix” composed of spatial displaced values as a key to artwork documentation is founded on holography interferometry (HI) principle^[31]. HI can obtain whole-field image of high information content in quantitative manner from complex and inhomogeneous artworks difficult to assess with other techniques and these results can be used as a reliable tool for artwork documentation through precise investigation protocols^[32-35]. The results are obtained from the interferometry fringe-pattern data formulated from induced surface displacements.

Holography and coherent metrology techniques are being used to measure the displacement, deformation and shape of solid mechanical objects and have been equally successful used in research of conservation of artworks^[36,40]. The techniques are based on optical path displacement of object points which are diffusely reflecting light towards the detector^[41].

A general purpose two-in-one basic HI hybrid experimental setup is shown in Fig. 1.

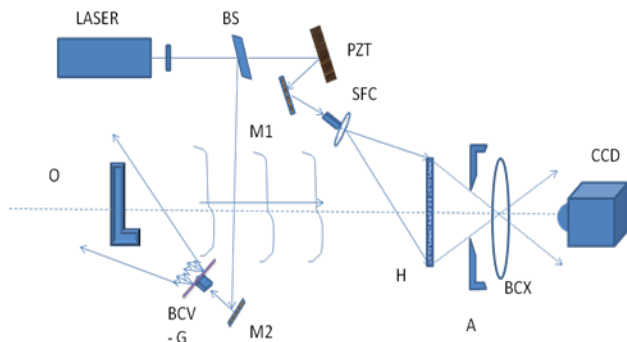


Fig. 1 An hybrid coherent geometry to capture an optical hologram from object O and its displaced position captured electronically in a holographic interferogram

BS: Beam Splitter, PZT: Piezoelectric Transducer, SFC: Spatial Filter Collimation, M: Mirror, H: Hologram Optical, A: Aperture, BCX: Biconvex Lens, BCV: Biconcave Lens Diffuser

The setup is a geometry arrangement to generate a master hologram of object O and a Holographic Interferogram (HI) from the displaced position of the object O. The basic geometry may vary considerably but to obtain the resolution of holographic modulation a reference beam is essential.

In this geometry the spatial displacement creating the interferogram is captured by a camera lens via the aperture A and the focusing lens BCX. To make a spatial coordinates record, many different geometries implying laser sources in interferometry designs are developed according to purpose^[42-45]. The laser beam is divided by a variable beam splitter (BS or VBS) into the reference (RB) and the object beam (OB). The reference beam is reflected upon a mirror mounted piezoelectrically controlled translator (PZT). The relative phase of the reference beam can thus be shifted in order to extract the phase from the interferogram by phase-stepping interferometry^[46,47]. The diffuse illumination of the object is achieved by the object beam passing first from a biconcave lens (BCV) and then through an optically random phase plate. The object is viewed through the hologram by a CCD-camera. The specularly reflecting object surface and the extended source (BCV- G) must be arranged so that all points on the object surface reflect a part of the diffuse illumination towards the hologram and the CCD-camera. In the setup shown, a ground glass plate (G) is employed as the random phase plate. There can be many variants of the described configuration in both beams and recording system with each variant offering advantages and disadvantages in the recording procedure^[48-50].

The challenge in designing an optical geometry for metrology purposes is to cope with the experimental objective and in particular in the Cultural Heritage with the required sensitivity for documentation and range of applications^[51]. Most artworks are considered diffusely reflecting objects, and are illuminated by a large divergence diffuse object wave.

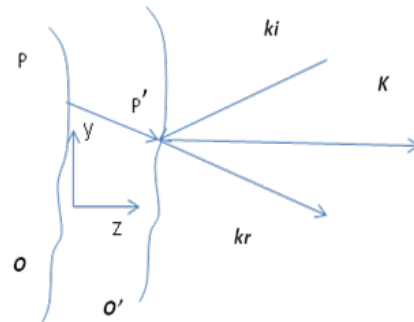


Fig. 2 A schematic of an object surface O displacement to O' position

Each infinitesimal surface area can be described by vector geometry of K_i : illumination vector, k_r : reflection vector, K : sensitivity vector

During a deformation, a point, p, on the object surface is displaced to a new point, p', see Fig. 2, and assume n points of the object surface have displaced to new position O', the corresponding phase shift of the reflected object wave is given by

$$\delta = d \cdot K \tag{1}$$

where $d = p' - p$ is the vector displacement of the surface and K is the sensitivity vector. The sensitivity vector K is determined by the difference between the wavevector of the incident wave, k_i , and the wavevector k_r , of the reflected wave from the surface, i.e.

$$K = k_r - k_i \tag{2}$$

The surface of the object is considered: i) to follow the laws of reflection so that the sensitivity vector K lies parallel to the local surface normal or in general case in the bisector of the angles; ii) the angles of the incident and the reflected wave obey the law of reflection; and iii) all points p of the surface

statistically reflect to the same direction towards the photosensitive medium, thus:

$$\mathbf{k}_r \cdot \mathbf{K} = -\mathbf{k}_i \cdot \mathbf{K} \quad (3)$$

Multiplying Eq. 2 by \mathbf{K} , using Eq. 3 and writing \mathbf{K} as $\mathbf{K} = Kn$ and $k_r = 2\pi/\lambda k_r$, yields the expression for the sensitivity vector:

$$\mathbf{K} = \frac{4\pi}{\lambda} (\hat{\mathbf{k}}_r \cdot \hat{\mathbf{n}}) \hat{\mathbf{n}} \quad (4)$$

where λ is the laser wavelength and \mathbf{k} , the unit vector in the viewing direction. Inserting the sensitivity vector in Eq. (1) the phase shift of the reflected wave causing the secondary fringes to appear becomes:

$$\delta = 2 \frac{2\pi}{\lambda} (\hat{\mathbf{k}}_r \cdot \hat{\mathbf{n}}) (\hat{\mathbf{n}} \cdot \mathbf{d}) \quad (5)$$

The expression for the phase change is leading to the expression for the Fizeau fringes^[52] where the geometrical condition of interference among non-coplanar or non-parallel plates is satisfied due to presence of two or more partially reflecting surfaces (4–30% reflectance). As such can be considered the two exposures required for the synthesis of a fringe pattern from the overlapping or the numerical reconstruction of two holograms to unwrapped phase maps.

The surfaces of artworks are other than parallel so the reflection properties should be considered in infinitesimal small angles for each single point as Fig. 2 schematically shows for one surface point^[53]. The statistical synthesis of each neighbor of surface point results to fringe contours of equal displacement used to assess the displaced surface. From Eq. 5 it is seen that the maximum sensitivity is achieved when the viewing direction is parallel to the plane that is vertical to the surface or in other terms to the surface normal. This out-of-plane configuration is most sensitive to the z-direction displacement towards which the deformation is manifested.

The dimensional changes in Cultural heritage objects are responsible for defects expressed vertical to the surface such as detachments between interfaces in multilayer composites eg panel paintings. These defects are commonly found in many types of artworks' construction independent of material composition varying from wall paintings, panel paintings, icons, polychromes, painted artworks, etc. to marquetry, furniture, decorative elements etc. These have in common that are objects made of more than one layer, characterized as multilayer construction, thus many layers are on top of bulk materials in order to achieve the desirable aesthetic appearance of the artwork. The most important issue for conservation practices is that the interface irregularities are not detectable unless they get irreversible macroscopic dimensions.

When measuring on specularly reflecting surfaces as varnishes, the direction of the sensitivity vector is always parallel to the local surface normal, regardless of the viewing and the illumination angle. This differs from the well-known situation where a diffuse scattering object surface is illuminated by a plane or a spherical object wave. In this situation the size and direction of the sensitivity vector are determined by both the illumination angle and the viewing angle, but is independent of the direction of the surface normal. In the special case of a plane object surface and equal angles of illumination and scattering/reflection, the two situations become identical.

By comparing two holograms of an object recorded at different deformation states, a pattern of interference fringes is formed as a result of the optical path difference between the two states. The use of CCD cameras can replace photosensitive mediums avoiding the time consuming wet processing. The resolution $R=(1.22\lambda)/2NA$ however depends on Numerical Aperture which decreases with NA increase in image-plane recordings. The lensless holographic interference is replaced by the speckle modulated interference with characteristic speckles of b dimensions, sizes determined by the aperture of the lens $b_s=1.22\lambda(f/D)$ with the Nyquist theorem requiring 2.3 pixels per point to resolve two closely spaced points. This translates into a pixel size of $R/2,3$. Nowadays with average pixel sizes of $6,5 \mu\text{m}$ and for $\lambda=0.532\mu\text{m}$ and setting $\#F=8$, $b_{sp}=2.44\lambda f/D=2.44\lambda F$ provide resolution $b_s=10.38\mu\text{m}$ among resolvable surface points and an average of 1.8 pixels per finite surface point is required. The holographic images are recorded onto a CCD detector (1024x1024) and digitally stored in a computer. The phase difference of the interference between the two images is numerically reconstructed^[59].

For the HI case, holograms of the object are recorded at two different times t_1 and t_2 after an optical path displacement is introduced due to an induced load that displaces the object from position O to O' . An intensity distribution in form of fringe pattern results from the optical path difference between the two holograms. This fringe pattern has the spatial information of surface points and is needed to quantitatively evaluate the amount of the static or dynamic deformation amplitude and phase, or to qualitatively assess the actual object shape. The introduction of a digital high speed acquisition system means that quite fast changing events can be studied and also that the system may be taken out of the laboratory-controlled environment.

IV. EXPERIMENTAL PROCEDURE PROOF OF PRINCIPLE

In the following examples the recording geometry is based on digital holographically modulated phase shifted interference of speckle patterns developed for interferometry application on art work research and on-field investigations. In Fig. 3 it shows the optical recording geometry.

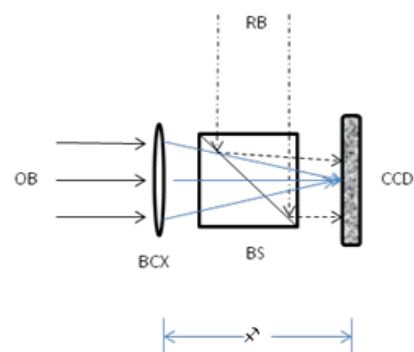


Fig. 3 Optical geometry of recording system, RB: Reference beam, OB: Object beam, BCX: Biconvex lens, BS: Beam Splitter, CCD: Coupled Charge Device

The damage factors can be identified from surface coordinates of structural displacement and are termed defects. The direct and contactless examination of surface as a function of time supports the concept to develop comparative routine investigation protocols for retrieval of spatial coordinates provided by optically coherent laser interferometry technology within art conservation field^[58].

In order to test as timeless the method of documentation through one-dimensional measurement of spatial coordinates, a technical sample in simple construction without defects is forced to change from one environment to another while surface changes are recorded at interval times $t=0.31, 0.43, 2.20, 3.18, 3.47, 4.45$ min. The fringes are generated and recorded at each six interval times. The positions are digitally registered and matrixes of coordinates corresponding to fringe number provide tables of the value of displacement in directions of sensitivity.

In this context multifunctional metadata have been generated from: a) numerical reconstruction of wrapped phase b) registration of x, y coordinates for each pixel position of each single stored fringe pattern as visually usable at any later time for comparison purposes; c) tables of defect trace localisation with sizes in coordinates and further post-processing routines with analysis; d) defect 2D topography and risk priority maps; and e) processing of unwrapped phase of fringe patterns with 3D map of deformation values.

The fringe intensity distribution $[cos(x)=sin(\pi/2+X)]$, per randomly chosen coordinate position upon surface reactions of technical sample is shown in four graphical representations a-d, Fig. 4 a-d. Six graphs across a constant x axis of surface are drawn in each of a-d. In graph (a) constant x at position $x: 354$, at (b) $x: 426$, at (c) $x: 547$, and (d) $x: 609$. Each x is evaluated from six responses in time a t_n ($t=0.31, 0.43, 2.20, 2.18, 3.47, 4.45$ second) starting from t_0 ($\Delta t=t_n-t_0$), and with varying y while the sample undergoes natural surface change.

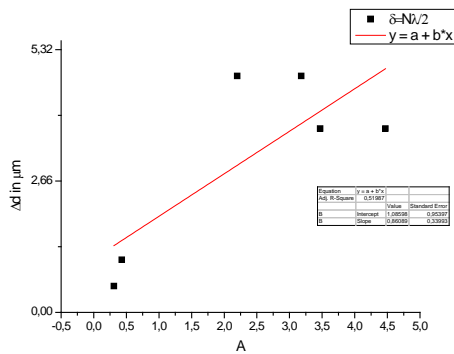


Fig. 4 Normalised intensity profiles showing spatial displacement of surface retrieved phase-wrapped fringe data

B. Controlled Alteration on Artwork Samples

In order to prove the method of spatial coordinates as timeless documentation in real artwork cases, the method of detection of known defects is used [64]. The experiment should provide detectable changes in micrometer scale within a time period in which any natural damaging effect couldn't have any detectable influence. In this context aging of technical samples is essential.

Typical technical samples simulating painted multilayered wood icons as artworks with induced structural particularities as defects are constructed to follow an artificial aging protocol¹ aiming to produce stimulated aging in short period. Aged samples with known defects are expected to react fast in externally induced disturbances. Table I presents an example of defects induced in the constructed samples.

According to literature, with simple heating at $102 \pm 3^\circ\text{C}$, the maximum deformation, at all directions (3 dimensions), would take place, due to the loss of the contained "natural"

moisture^[54-56]. This type of ageing could be described as oxidation. Although the other deterioration mechanisms of lignin, i.e. hydrolysis and photooxidation, are theoretically not introduced to the samples by this procedure, the macroscopic results on the structure simulate the condition of old paintings on wood such as post-Byzantine icons. An accelerated ageing procedure in a stove (Memmert Company) with maximum air recycling is performed. The indoor relative humidity varies from 45 to 50% during the whole procedure. Stimulated aging is performed under the aging protocol to initially reach 73 years of aging. Samples are examined prior the ageing and after two ageing cycles.

TABLE I SAMPLE CONSTRUCTION¹

Sample	Layer	Defect
Byzantine icon	Wooden substrate	knots
	Textile;	
	preparation layer (gesso+animal glue)	loss of ground layer
	Bole	
	layer of gold	partial loss of gilding
	Paint layer (pigments + egg yolk)	
	Varnish	

C. Acquiring the Reference State

As reference state is considered hereafter the spatial displacement recorded via the interferometry geometry at the first examination of the icons under an experimentally controlled load that provokes dimensional displacement. The whole object is displaced a distance, d , in the z -direction from its initial position and the first measurement is taken.

As can be seen in Fig. 2 the object surface is displaced an optical path change is introduced. The optical path change corresponds to a measurable quantity with the optical distance d being an integer multiple of $\lambda/2$, so that $d = N \cdot \lambda/2$, N integer. In acquiring the reference state the induced optical path displacement is used for the whole surface of the artwork. The first measurement is taken at reference position and the sequence of measurements with the whole object displaced at a distance, S , from its initial position.

If the entire object gets same quantity of induced change replies with a whole-field displacement, thus the displacement, d_0 , is common to the entire surface and the fringes describe the displacement. Displacement in x, y direction is visualised as parallel or strain fringes and in z as circular or concentric. If the object includes structural discontinuities, as in the case of the induced defects in the Byzantine icon sample, the displacement is not common to the entire surface and the fringes change direction tracing the discontinuous presence.

The surface topography can be calculated from the measured surface normal to x, y orthogonals or to z direction from the 0 order fringe as it terms the 0 displacement field of the steady or non-displaced object points. The zero-order is

¹ *Constructino and ageing of Byzantine icon sample performed by Dr Eleni Kouloumpi, head of science conservation department of National Gallery of Athens Alexandros Soutzos Museum, for the R&D Annex of MultiEncode project (EC funding SSP1-00006427)*

easily identified by a localized increase in intensity measurements via a photometer. If there are defects which are displaced randomly then these defects cause irregularities in the surface topography since the 0 to 0' position is not equal for all object surface points. The produced fringe pattern irregularity is directly visualizing the effect on the surface localizing the defect with local number of fringes being distinct from the whole field number of fringes.

D. Acquiring the Comparison State

For the comparison state a displacement, S, of the whole surface is required and according to the type of load the direction of displacement is expected. Ageing is performed in conservation labs. It is assumed that the ageing has produced changes in the structure of the icons.

If the entire object gets same quantity of induced change replies with a whole-field displacement $\mathbf{d}_1 \neq \mathbf{d}_0$ different from the reference state, the same $\mathbf{d}_1 \neq \mathbf{d}_0$ applies for the displacement in case of the known induced defects. Interference fringe distribution is assessed by intensity profiles across wrapped interferogram phase of reference-comparison states.

Localised fringe patterns produce inhomogeneous intensity values across the intensity profiles and x, y coordinates are extracted in position registering tables. To quantify the localized patterns the surface topography method is used. By measuring three values of the phase shift corresponding to three displacements, \mathbf{d}_i $i = 1, 2, 3$, a set of three phases for the three components of the surface normal Eq. 5 can be solved with N getting values of fringe numbers accordingly. A simple solution is found by choosing the set of \mathbf{d}_i to be three orthogonal displacements in directions parallel to the axes of a Cartesian system of coordinates. The system of coordinates is chosen with the z-axis parallel to the viewing direction, \mathbf{k}_z . The three components of the surface normal, $n(x, y)$, each defect is determined from three measurements providing the exact localization of each.

E. Reference State to Comparison State Assessment

In optical metrology applications the deformation plot resulted after the post-processing of phase unwrapped fringe-data is used to visualise the induced surface change. In this application the assessment starts before the fringe post-processing analysis and the unwrapped phase. The spatial-coordinates of the phase wrapped fringe-data is the first data-source in the documentation. The physical analytical method can be described in terms of the analogue method of real-time speckle interferometry^[57] in which the accurate repositioning of the reference record of surface speckled-pattern with the comparison state allowing the generation of interferometry fringes among the two states solely depend on the amount of speckle correlation.

If the object on the comparison state is fully correlated to the reference state no interference appears, if in the comparison state it has been translated by an amount L so that $\delta = (2N + 1)\pi$ a degree of uncorrelation between speckle patterns which modulates interferometrically the object surface is observed. The fringes outline regions of the object which have the same component of displacement, normal to the bisector of interfering beams Fig. 1, and lying in the plane containing \mathbf{k}_1 and \mathbf{k}_2 (reference-comparison directions).

In this methodology the resulted fringe patterns are holographically modulated and the speckle patterns become

sensitive to normal displacements. The out-of-plane direction is mostly important for complex organic structures of artworks due to dimensional expansion. Hence the addition of the coherent reference wave in the z direction of the speckle field via a combiner beam splitter changes the relative phase in displacement direction Δz , so $\Delta\varphi = \frac{2\pi}{\lambda}(1 + \cos\theta_1)\Delta z$. As the surface moves in axial direction uncorrelation of speckles appear in $\Delta z = \frac{N\lambda}{1 + \cos\theta_1}$, with $N=0, \pm 1, \pm 2, \dots$, Eq. 6.

While the speckle pattern is unchanged and fully correlated if $\Delta z = \frac{(N + \frac{1}{2})\lambda}{1 + \cos\theta_1}$, with $N=0, \pm 1, \pm 2$, this allows x, y, z spatial coordinates of object surface to be recorded in fringe patterns speckle irradiance distribution or speckle interferogram with spatial resolution comparable to holographic interferometry.

To avoid speckle decorrelation during experimental recordings the relative displacement should be experimentally controlled by an induced stepwise incrementally increased load. For the same reason in the presented application that a comparative in future time measurement is required, the object maintenance should be kept under control to avoid excessive deterioration.

V. RESULTS

A. Proof in Technical Sample with Known Defects

In Fig. 4 it shows extraction of intensity profiles values from the reference state at time t_0 . Surface responses is recorded in form of phase wrapped cosinusoidal interference fringes. Fringe distribution values are extracted in randomly chosen normalised intensity profiles shown in Figure 4 to provide access to the spatial coordinates indicating the displacement from each distinct surface position.

The technical sample used was fixed in one position while the surrounding environment was changing^[59]. The graphs are taken across constant x axis with varying y at different t_n from t_0 ($\Delta t = t_n - t_0$), while sample undergoes the natural surface change. The dimensional displacement generates a fringe pattern similar to the thermal expansion pattern of circular fringe distribution. Due to material unhomogeneities the centre of the circle is originating with axial y asymmetry as shown in the normalised graphs. The asymmetry depends on fringe density, in coordinate x: 354 that is closer to the centre of the sample and in graphs of $t=0.31$ the asymmetry is shown from pixel 250 to 1000 and for $t=0.43$ sec from pixel 300-1000, and shrinks variably as the fringe density increases with time. There is also decrease in fringe distance evidential of unknown defect in the position 220-250 shown well in coordinate x: 426 for $t=0.43$ s and x: 547 at $t=0.31$ s, $t=3.47$ s, and for x: 609 the normalised graphs still shows evidence of affected fringe distribution at $t=0.31$, $t=0.43$, $t=2.20$, $t=3.18$ and $t=3.47$ at pixels from 480-520. A known defect instead can be localised at near 500 pixel position for most t and in coordinates from x: 426, x: 547, x: 609.

The length of the known defect is found by the coordinate x,y and is registered as 1.48 cm in x and 1.70 in y direction, while the unknown defect is registered as unstable among 1.1 to 1.5 cm in x,y accordingly. This observation allows the following hypothesis: the known defect appears mostly stable

in regards to the effect that produces on the surface while the unknown defect produces unstable effect. This indicates that different defects can be differentiated from the effect the surface as dynamically stable or dynamically unstable as the in-growth defects [60-63].

According to Eq. 6 a range of displacement for each t and for random choice coordinates along y with constant x is summarised in Table II:

TABLE II MEASURED DISPLACEMENT FOR RANDOM COORDINATES AT VARYING T

Time (sec)	y: 354	y:426	y:547	y:609
0.31	0.532	0.532	0.532	0.532
0.43	1.064	1.596	1.064	1.064
2.20	4.788	6.384	6.916	6.916
3.18	4.788	4.256	6.384	5.852
3.47	3.724	5.320	5.320	4.788
4.47	3.724	3.724	3.724	3.724

Documentation in terms of spatial coordinates is allowed and sets of spatial coordinates eg $x_1.y_c: 354,500$ $x_2.y_c: 426,500$ $x_3.y_c: 547,500$ $x_4.y_c: 609,500$ and for any x, y corresponding to pixel intensity values 0-255 in times t_{0-n} for a unique record of the investigated artwork is formed. A retrievable and known intensity modulation representing surface point fluctuations and phase change alteration is registered. In the presented examples the phase fluctuation for majority of points is $>\pi/2$ in consequent records witnessing the structural stability of surface.

The fringe density if plotted as the sum of displacement in transient process of surface alteration increases linearly with time as seen in graphs shown in Fig. 5.

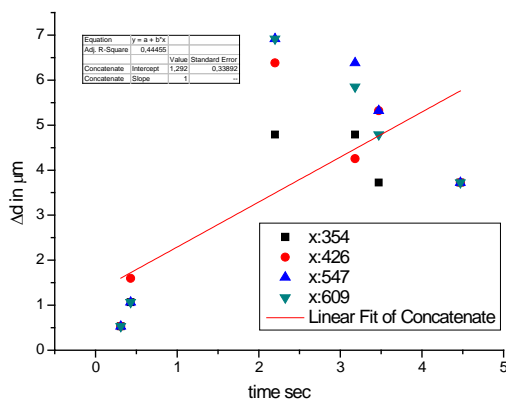


Fig. 5 Linear increase of fringe density with time

Since as basis to the compared next values is used the first reference value of the phase-shifted interferometric time-interval of surface change then the generalized increase seen in graphs it shows an expected ongoing process.

For the displacement of surface points across chosen coordinate, the plot follows the fringe intensity fluctuation visualizing the deformation across the line as seen in graphs of Fig. 6.

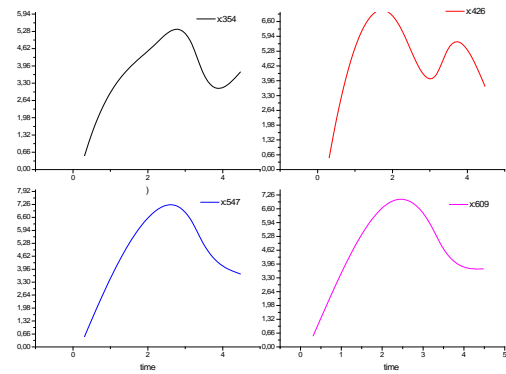


Fig. 6 Surface response in selected time intervals to a range of coordinates

In the graphs in Fig. 6 it is evident that the surface response in the selected time intervals differs to the range of coordinates while the variations in density is expected since the surface is deformed randomly and coordinates are randomly chosen corresponding to different regions of the object surface. The observed increase in density in graphs is related to coordinates with higher slope.

The asymmetry in distribution is observed in some coordinates located further far from the centre of generated circular fringe pattern. The deformation trend of surface at times t_{0-n} for a unique record of the investigated artwork is registered to complete artwork “fingerprint” documentation. In case of defects visualized through local asymmetry distributions, they are separately traced and processed. For comparison identification purposes the information is stored in database. An exemplary table is shown in Table III.

TABLE III DEFECT REGISTRATION

Number of Area/Defect	Direction Measured	Size	Coordinates
No_1	x	1.48 cm	354,500 to 609, 500
No_1	y	1.7 cm	354,500 to 354, 733
No_1	z	1.2 μm	as in No_1 x,y

The database registers through coordinate sets of the examined area, each intensity profile, size and deformation corresponding to a set of critical boundary conditions.

B. Proof in Icon Case Sample

The icon samples with artificial aging are then investigated before and after the ageing process with time interval ensuring higher temporal separation among the reference and comparative states. The sample was examined before the ageing and then has undergone an ageing process that simulated 72 years of ageing (Heating at intervals at 102°C, for totally 66.5 hrs in two cycles of ageing process).

Following the same experimental procedure as in prior to ageing examination that provided the reference state, in simulation terms 72 years ago, the new comparative positions are acquired. The coordinates showing known defects are located and new profiles are extracted and sized. Fig. 7a, b shows the surface responses obtained before the simulation of ageing of 72 years from phase wrapped maps in form of cosinusoidal interference fringes extracted in normalised

intensity profiles to provide the displacement in spatial coordinates for the one dimensional measurements.

experiments and it is expressed in the high increase in relative displacement values.

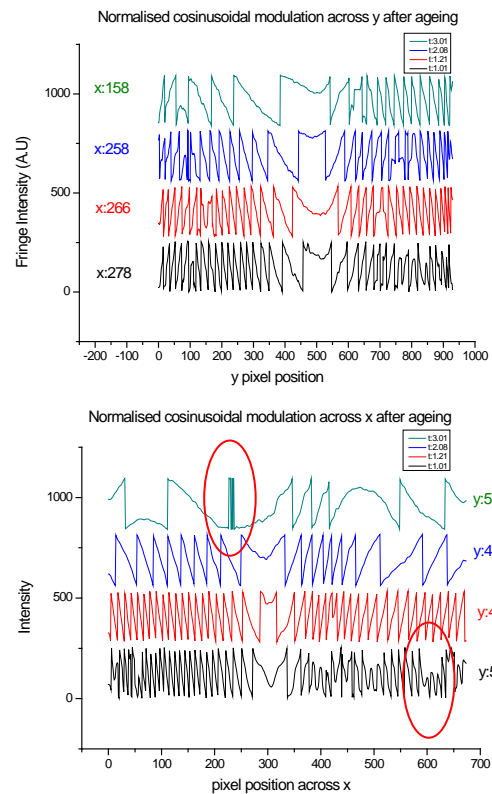
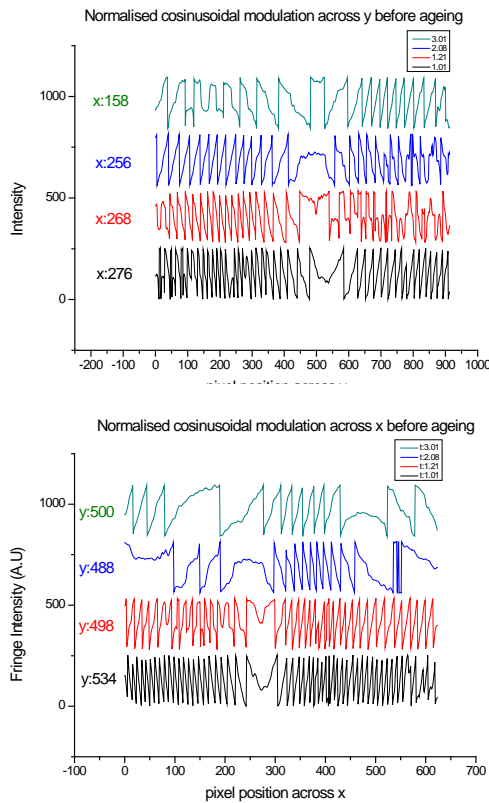


Fig. 7 Before ageing: Icon surface responses in form of phase wrapped cosinusoidal interference fringes extracted in normalised intensity profiles providing the spatial coordinates' displacement

Fig. 8 After ageing: Icon surface responses in form of phase wrapped cosinusoidal interference fringes extracted in normalised intensity profiles providing the spatial coordinates' displacement

The graphs are taken a) across constant x axis with varying y and b) across constant y with varying x, at different t_n from t_0 ($\Delta t = t_n - t_0$) while sample undergoes induced surface change

The graphs are taken a) across constant x axis with varying y and b) across constant y with varying x, at different t_n from t_0 ($\Delta t = t_n - t_0$) while sample undergoes induced surface change, sample has been aged in conservation ageing

The graphs are taken across constant value at x axis with varying y and across constant y with varying x, at different t_n from t_0 ($\Delta t = t_n - t_0$), while sample undergoes natural surface change. The modulated interference fringe distribution before ageing is expressed with expected circular fringe generation located at the centre as can be seen at coordinate x:300, y:500 for Fig. 7b and 7a correspondingly. Hence before ageing is not retrieved any dominant asymmetry.

The displacement has been again calculated for the various t_{0-n} for both x, y axes before and after the ageing process for the different coordinates, as shown in Table IV:

TABLE IV MEASURED DISPLACEMENT FOR RANDOM COORDINATES AT VARYING T

Time (Sec)	Before Ageing across X	Before Ageing across Y	After Ageing across X	After Ageing across Y
1.01	14.364	11.704	14.896	12.108
1.21	11.172	10.64	11.704	9.044
2.08	4.788	7.980	5.320	8.512
3.01	3.724	5.862	3.192	5.852

After the ageing processes material inhomogeneities are dominantly expressed and can be seen at Figure 8. The centre exhibits axial x mostly asymmetry as shown in the normalised graphs across position x. At position across y is observed a shift of central peaks to the left evidenced with the different x coordinate, since exemplary x,y coordinates were chosen to cross the centre of thermal expansion. Observing the micrometric shift of coordinates before and after ageing the different responses of surface points become apparent and any shift is retrieved, localised, sized and isolated to pinpoint and identify the corresponding artwork region in time.

Thermodynamically the linearity in fringe density is expected since the unloading cycle forces the icon to react faster in the start of the physical process in order to achieve equilibrium with the environment. The surface tends to slow the reaction in accordance to the decrease of thermal differences and finally to reach equilibrium. Thus the displacement value is decreased with time. The slope of deformation remains proportional before and after ageing cycles with the after ageing cycle exhibiting coordinates shift and marginally higher displacement values. It is locally

In contrast to the technical sample and the measurements with small time intervals of graphs in Fig. 5, in graphs Fig. 7 and Fig. 8, the surface responses vary considerably indicating defects and structural instability. The induced thermal load provokes higher value of surface reaction at the start of the unloading process compared to the natural upload of previous

witnessed distortion on fringe distribution indicating evidence of structural instability and risk for deterioration in terms of generation of defects. It is seen in the case of x: 225, y: 500 where a steep phase change in consequent fringes is taking place and a crack is exhibited. At x: 100 y: 488 to x: 200 y: 488 the constant fringe intensity parallel to axis is the evidence of detachment growth. Some coordinates remain comparable but the coordinates at y: 500, at y: 488 before and after ageing are distorted across axis and is difficult to find one surface point reacting in same values as before ageing. Thus the corresponding points of the profiles are registered as instable and correlated to the artwork actual surface areas produce an updated documentation of risk.

VI. DISCUSSION

In this paper a feasibility experiment to exploit and implement spatial 1d-2d data as derived from interferometry fringes for surface authentication and impact analysis was performed. It is confirmed that intensity profiles across cosinusoidal fringe distribution exhibit the surface point fluctuations and can be implemented to register structural information with a resolution of average 10 μm or sharper depending on the recording geometry and medium settings as interference angle, recording medium, pixel size and numerical aperture.

The intensity profile data reveal the extent of fringe fluctuation and distortion which can be used to assess the total surface reaction and unknown inhomogeneities or defect growth and deterioration. It also seems to be possible to differentiate from the slope of fringe change the type of defect. The 2D dimensional data are interference-fringe sensitive holding the advantage of a highly secure and anti-fraud method with the disadvantage of requiring routine database update.

Interferometry visual data are very unique and important due to high information content and resolving capabilities. However the usual fringe pattern data are cumbersome for human eye and automatic post processing is not yet applicable to the art conservation field due to the complexity of objects which generates highly distorted fringe patterns. Intensity profiles hold potential for fringe interpretation and analysis by a scholar while hold potential to aid to the effort of automisation especially in relation to the complex problems of phase-unwrapping in art conservation field. It should be noted that application on industrial materials or typical engineering objects do produce less complexity of fringe patterns due to material homogeneity.

Therefore exploring in art conservation research the unique structural information provided by coherent interferometry for which known commercially available software fail to respond it is a dedicated field of research addressed in the presented research paper.

ACKNOWLEDGMENT

Most of the research was carried out during the project MULTIENCODE-006427. The work is on-progress and Climate for Culture- 226973 and CHARISMA- 228330 projects are equally acknowledged for the continuation of funding.

REFERENCES

- [1] C. Cennini, *The craftsman's handbook: translation of Il libro dell'arte*, trans. D. Thompson (Dover Publications New York 1960).
- [2] Theophilus, *Diversarum artium schedula (On divers arts: the treatise of Theophilus)*, trans. J. Hawthorne and C. Smith, (University of Chicago Chicago 1963).
- [3] G. Thomson, *The Museum Environment 2nd ed.*, (Butterworth-Heinemann 1990).
- [4] W. Simpson, "Wood handbook : wood as an engineering material", Madison, WI : USDA Forest Service, Forest Products Laboratory, 1999.
- [5] S. Rivers, N. Umney, *Conservation of Furniture*, (Butterworth-Heinemann London 2003).
- [6] G. Tsoumis, *Science and Technology of Wood. Structure, Properties, Utilization* (Van Nostrand Reinhold New York 1991).
- [7] Glenn F. Knoll, *Radiation Detection and Measurement*, Chapter 1, Page 1, John Wiley & Sons; 3rd Edition.
- [8] Huang, D; Swanson, EA; Lin, CP; Schuman, JS; Stinson, WG; Chang, W; Hee, MR; Flotte, T et al. (1991). "Optical coherence tomography." *Science* 254 (5035): 1178 – 81.
- [9] Bourquin, S.; Seitz, P.; Salathé, R. P. (2001). "Optical coherence tomography based on a two-dimensional smart detector array". *Optics Letters* 26 (8): 512.
- [10] Dunsby, C; Gu, Y; French, P (2003). "Single-shot phase-stepped wide-field coherence gated imaging." *Optics express* 11 (2): 105 – 15.
- [11] Structural Examination of Easel Paintings with Optical Coherence Tomography, Piotr Targowski, Magdalena Iwanicka, Ludmila Tymiska-Widmer, Marcin Sylwestrzak and Ewa A. Kwiatkowska, *Acc. Chem. Res.*, 2010, 43 (6), pp. 826 – 836.
- [12] Kaufman, S. Musch, DC. Belin, MW. Cohen, EJ. Meisler, DM. Reinhart, WJ. Udell, IJ. Van Meter, WS "Confocal microscopy A report by the American Academy of Ophthalmology". *Ophthalmology* 111 (2): 396, (2004).
- [13] Pawley JB (editor) (2006). *Handbook of Biological Confocal Microscopy* (3rd ed.). Berlin: Springer. ISBN 038725921 (2006).
- [14] Multispectral general sources.
- [15] V. Papadakis, A. Loukaiti, P. Pouli, "A spectral imaging methodology for determining on-line the optimum cleaning level of stonework", *J. Cult. Heritage*, 2010, 11, 325-328.
- [16] Peng, T., Gupta, S.K.: Model and algorithms for point cloud construction using digital projection patterns, *Journal of Computing and Information Science in Engineering*, 7(4): 372 – 381, 2007.
- [17] Contribution by various authors on Fringe 2005, The 5th International Workshop on Automatic Processing of Fringe Patterns Berlin: Springer, 2006.
- [18] R. Jones, The design and application of a speckle pattern interferometric for total plane strain field measurements, *Opt. Laser Technol.* 8, 215 – 219, 1976.
- [19] C. Young, Quantitative measurements of in-plane strain of canvas paintings using ESPI, *Proceeding of the Applied Optics Division, IOP Publishing, Brighton*, 79 – 84, 1998.
- [20] Leith E. N. and Upatnieks J., *Wavefront reconstruction with diffused illumination and three-dimensional objects*. *J. Opt. Soc. Am.*, 1964. 54: p. 1295 – 1301.
- [21] Haines K. A. and Hildebrand B. P., *Surface deformation measurement using the wavefront reconstruction technique*. *Appl. Opt.*, 1966. 5: p. 595 – 602.
- [22] V. Tornari, "Laser Interference-Based Techniques and Applications in Structural Inspection of Works of Art", *Analytical and Bioanalytical Chemistry*; 387, 761 – 80 (2007).
- [23] V. Tornari, A. Bonarou, V. Zafiropoulos, C. Fotakis, N. Smykakis, S. Stassinopoulos, *J. Cult. Heritage* 4, 347s (2003).
- [24] R. Jones & C. Wykes, *Holographic and Speckle Interferometry*, 1989, Cambridge University Press, Cambridge, UK.
- [25] J. C. Dainty ed. *Laser Speckle and related phenomena*, Springer Verlag, Berlin 1975.
- [26] E. Tsiranidou, V. Tornari, Y. Orphanos, C. Kalpouzou, M. Stefanaggi, "Time-dependent defect reveal assessed by combination of laser sensing tools", In the Proceedings of the 6th International Conference on Lasers in the Conservation of Artworks (LACONA VI), Series Eds. J. Nimmrichter, W. Kautek and M. Schreiner (Springer Proceedings in Physics 116, 2007), 611 – 620.
- [27] Gulker, G., Hinsch, K., Holscher, C., Kramer, A., and Neunaber, H., *In-situ application of electronic speckle pattern interferometry (ESPI) in the investigation of stone decay*, *Proc. SPIE / Laser Interferometry: Quantitative Analysis of Interferograms*, 1162, 156 – 167, 1990.
- [28] Hinsch, K.D., T. Fricke-Begermann, G. Gulker, K. Wolf, Speckle correlation for the analysis of random processes at rough surfaces, *Optics Lasers Eng.*, 33, 87 – 105, 2000.

- [29] Marc P. Georges, Véronique S. Scauflaire, Ph. C. Lemaire, "Compact and portable holographic camera using photorefractive crystals. Application in various metrological problems", *Appl. Phys. B* 72, p. 761 – 765 (2001).
- [30] Marc Georges, Cédric Thizy, Véronique Scauflaire, Sébastien Ryhon, Gilles Pauliat, Philippe Lemaire, Gérald Roosen, "Holographic interferometry with photorefractive crystals : review of applications and advances techniques", *Proc. SPIE Vol. 4933 on Speckle Metrology 2003*, p. 250 – 255.
- [31] *Holographic Interferometry*, C.M. Vest, (John Wiley & Sons New York 1978).
- [32] V. Tomari, E. Bemikola, W. Osten, R.M. Grooves, M. Georges, T. Cedric, G.M. Hustinx, E. Kouloumpi, A. Moutsatsou, M. Doulgeridis, S. Hackney, T. Green. "Multifunctional encoding system for assessment of movable cultural heritage", In the Proceedings of the 7th International Conference on Lasers in the Conservation of Artworks (LACONA VII), Series Eds. Castillejo et al., Taylor and Francis group, London, (2008).
- [33] V. Tomari, Y. Orphanos, R. Dabu, C. Blanaru, A. Sratan, O. Pacala, D. Ursu, "Non-destructive speckle interferometry diagnosis method for art conservation", International Conference Advanced Laser Technologies ALT'06, Sept. 8 – 12, 2006, Brasov, ROMANIA, SPIE volume 6606.
- [34] E. Bemikola, V. Tornari, A. Nevin, E. Kouloumpi, "Monitoring of changes in the surface movement of model panel paintings following fluctuations in relative humidity; preliminary results using digital holographic speckle pattern interferometry", In the Proceedings of the 7th International Conference on Lasers in the Conservation of Artworks (LACONA VII), Series Eds. Castillejo et al., Taylor and Francis group, London, (2008).
- [35] V. Tomari, E. Bemikola, W. Osten, R.M. Grooves, M. Georges, G.M. Hustinx, E. Kouloumpi, M. Doulgeridis, S. Hackney, T. Green, "Coherent metrology in impact assessment of movable artworks", CHRESP 8th European Commission Conference on Sustaining Europe's Cultural Heritage, Ljubljana Slovenia 10 – 12 November 2008.
- [36] Amadesi S., D' Altorio A., and Paoletti D., *Real-time holography for microcrack detection in ancient golden paintings*, *Optical engineering* 22(5), 660 – 662 (1983).
- [37] Ambrosini D. and Paoletti D., "Holographic and speckle methods for the analysis of panel paintings, developments since the early 70s", *Reviews in Conservation* 5, 2004, 38 – 48.
- [38] V. Tomari, A. Bonarou, E. Esposito, W. Osten, M. Kalms, N. Smyrnakis, S. Stasinopoulos, "Laser based systems for the structural diagnostic of artworks: an application to XVII century Byzantine icons", SPIE 2001, Munich Conference, June 18 – 22, 2001, vol. 4402.
- [39] A. Bonarou, V. Tomari, L. Antonucci, S. Georgiou, C. Fotakis, "Holographic interferometry for the structural diagnostics of UV laser ablation of polymer substrates", *Appl. Physics A*, vol. 73, pp. 647 – 651 (2001).
- [40] A. Athanassiou, E. Andreou, A. Bonarou, V. Tomari, D. Anglos, S. Georgiou, C. Fotakis, Examination of chemical and structural modifications in the UV ablation of polymers, *Applied Surface Science* 197 – 198 (2002), 757 – 763.
- [41] Hansen, R. S. & Hassing, S., Deformation measurement of specularly reflecting objects using holographic interferometry with diffuse illumination, *Proceedings of the SPIE International Conference on Optical Holography*, ed. T. Honda, (1995) 2577, pp. 218 – 25.
- [42] Wykes, J.N. Butters and J. A. Leendertz, *Journal of measurement and control*, 4, 344 – 350, (1971).
- [43] R.K. Erf (ed) *Speckle Metrology*, Academic Press, New York, 1978.
- [44] E. Hecht and A. Zajac, *Optics*, Addison-Wesley, Reading, MA, 1974.
- [45] Rastogi P.k. ed, *Digital Speckle Pattern Interferometry & Related Techniques*, Wiley, New York, 2000.
- [46] Schürner, J., Etemeyer, A., Neupert, U., Rottenkolber, H., Winter, C. & Obermeier, P., New approaches in interpreting holographic images. *Optics and Lasers in Engineering*, 14 (1991), 283 – 291.
- [47] Yura, H. T., Hanson, S. G. & Grum, T. P., Speckle: statistics and interferometric decorrelation effects in complex ABCD optical systems. *J. Optical Society, A*(1) (1993), 316 – 323.
- [48] G. Pedrini, H.J. Tiziani, Y. Zou, Digital double-pulse TV holography, *Opt. Lasers Eng.* 26, (1997), 199 – 219.
- [49] R. Rodriguez Vera, D. Kerr, F.M. Santoyo, Electronic Speckle Contouring, *J. Opt. Soc. Am. A* 9, (1992), 2000 – 2008.
- [50] Staffan Schedin, Giancarlo Pedrini, Hans J. Tiziani, Fernando Mendoza Santoyo, All-fibre pulsed digital holography, *Optics Communications* 165, (1999), 183 – 188.
- [51] *Lasers in the Preservation of Cultural Heritage; Principles and applications*, Fotakis C., D. Anglos, V. Zafiropoulos, S. Georgiou, V. Tornari, Ed. R. G. W. Brown, E. R. Pike (Taylor and Francis, New York 2006).
- [52] Hansen, R. S. & Hassing, S., Deformation measurement of specularly reflecting objects using holographic interferometry with diffuse illumination, *Proceedings of the SPIE International Conference on Optical Holography*, ed. T. Honda, (1995) 2577, pp. 218 – 25.
- [53] *Optics*, Klein, T. & Furtag, E., Wiley, New York, (1986).
- [54] *Cellular ultrastructure of woody plants*, Côté W. A. Jr., (1965), Syracuse University Press, Syracuse, N. Y., pp. 602.
- [55] *Accelerated Aging*, Feller R. L., (1994), The Getty Conservation Institute, pp. 162.
- [56] *Επιστήμη και Τεχνολογία του Ξύλου (Science and Technology of Wood)*, Tsoumis T. G., (1983), Thessaloniki, pp. 655.
- [57] J.A. Leendertz, Interferometric displacement measurement on scattering surfaces utilizing the speckle effect, *J. Phys. E. Sci. Instrum.*, 3, 214 – 218 (1969).
- [58] V. Tornari, E. Bemikola, A. Nevin, E. Kouloumpi, M. Doulgeridis, C. Fotakis, "Fully non contact holography-based inspection on dimensionally responsive artwork materials". *Sensors* 2008, 8, DOI 10.3390/sensors.
- [59] E. Bemikola, A. Nevin, V. Tomari, "Rapid initial dimensional changes in wooden panel paintings due to simulated climate-induced alterations monitored by digital coherent out-of-plane interferometry", *Applied Physics A* 95, pp. 387 – 399 (2009).
- [60] V. Tomari, E. Bemikola, W. Osten, R. M. Grooves, G. Marc, G. M. Hustinx, E. Kouloumpi and S. Hackney, "Multifunctional Encoding System for Assessment of Movable Cultural Heritage", *Experimental Analysis of Nano And Engineering Materials And Structures* 2007, C, 18, 715 – 716, DOI: 10.1007/978-1-4020-6239-1_355.
- [61] V. Tomari, E. Bemikola, W. Osten, R. M. Grooves, G. Marc, G. M. Hustinx, E. Kouloumpi, M. Doulgeridis, T. Green and S. Hackney, "Coherent metrology in impact assessment of movable artwork: the MULTIENCODE project", 8th European Commission Conference on Sustaining Europe's Cultural Heritage, 10 – 12 November 2008, Ljubljana, Slovenia.
- [62] C. Thizy, M. Georges, M. Doulgeridis, E. Kouloumpi, T. Green, S. Hackney, V. Tomari, "Role of dynamic holography with photorefractive crystals in a multifunctional sensor for the detection of signature features in movable cultural heritage", *Proceedings of the SPIE Conference. Vol 6618 on O3A: Optics for Arts, Architecture, and Archaeology*, paper 6618 – 28, Munich, June 2007.
- [63] E. Bemikola, K. Hatzigiannakis, Y. Orphanos, E. Kouloumpi, V. Tornari, *Proceedings of the SPIE conference. "Development of impact assessment procedure and preliminary results with digital holographic speckle pattern interferometry for signatures multi-encoding use"*, Vol 6618 on O3A: Optics for Art, Architecture and Archaeology, 66180Z (2007); doi:10.1117/12.726173.
- [64] Interference fringe-patterns association to defect-types in artwork conservation: an experiment and research validation review, Vivi Tornari, Eirini Bernikola, Elsa Tsiiranidou, *Applied Physics A: Volume 106, Issue 2* (2012), Page 397 – 410.



Vivi Tomari (Athens, 1962) received her BSc in Optics-Physical Optics (NTEIA Optics), MSc in Material Science (NTUA Chemical Engineering), PeD on Holography (RCA Holography) MPhil/DPhil on Conservation Science (RCA/V&A/ICSTM), PhD (cand. NTUA). She is heading Holography laboratory at Institute of Electronic Structure and Laser in Foundation for Research and Technology Hellas since 1995. She is experienced coordinator of National,

International, and European research projects. She is the author and co-author in over 100 papers in peer-review journals, academic magazines, conference proceedings and text books. Research interests varying from applied physics and coherent metrology applications on artwork conservation field to include physics and mechanisms of laser-matter interactions and optical system developments to the philosophy of physics and specially to wave interference and interconnection of information.